Numerical Simulation of the Process of Autoregulation of the Arterial Blood Flow

N. A. Kudryashov and I. L. Chernyavskii

e-mail: kudryashov@mephi.ru

Abstract—For describing the autoregulation of the blood flow in an artery under constant transmural pressure a mathematical model that takes into account the multilayer structure of the arterial wall, the diffusion and kinetic processes in the wall, and the nonlinear viscoelastic properties of the wall material is proposed. The limiting case of a thin-walled artery is studied analytically. The arterial-wall viscosity range on which the equilibrium state of the system is stable is estimated. Accurate stationary distributions of the nitric oxide, calcium and myosin concentrations in the arterial wall are found. Numerical simulation of the autoregulation process demonstrated the possibility of arterial adaptation to radius perturbations, the existence of slow oscillations, and system transition to a new equilibrium state with change in blood flow level. The results are in good agreement with the experimental data.

A common approach to modeling the vascular system is to extend the classical hydrodynamic models of liquid flow through elastic tubes to the case of blood flow through arteries [1–3]. However, in some cases, for example, for resistive muscular arteries, it is necessary to take into account differences between the usual passive and the "biological" active tube [4].

The walls of arteries and arterioles contain smooth muscles which can contract or relax in response to nerve impulses and various factors of a mechanical or chemical nature, thereby regulating the vessel lumen and the blood pressure and flow-rate. There are two main mechanisms of local autoregulation. The first is the muscular tonus of the arterial wall due to the shear stress on its inner surface [5–8]. The second mechanism, which is determined by the sensitivity of the smooth-muscle tissue to the modification of the tensile stress by the blood pressure, is known as the Bayliss effect, or myogenic response [9, 10]. Moreover, there is a regulatory mechanism realized by means of the vegetative nervous system via the vessel-wall baroreceptors, which are sensitive to the transmural pressure [11].

Let the transmural blood pressure P_0 be maintained constant and the blood flow vary (see, for example, experimental investigation [5]). Then the first of the above-mentioned effects related with the shear stress plays the leading role.

In this study we will consider the effect of the shear stress on the blood vessel dilatation involving nitric oxide (NO), taking into account its diffusion and absorption, as well as biochemical reactions in the vessel wall [12, 13].

It was long assumed that the endothelial cells lining the inner surface of the arterial bed only isolated the blood from the wall tissues and reduced flow friction. However, in 1980 Robert F. Furchgott and coworkers showed [14, 15] that the endothelial cell layer plays a key part in the relaxation of the smooth muscles in the artery. Thus, an endothelium-dependent factor in vessel muscle-tissue relaxation was discovered. Following further investigation, the nitric oxide molecule was proposed as a signal molecule that connects the endothelium and the smooth muscles in the artery wall. The endothelium-dependent mechanism of
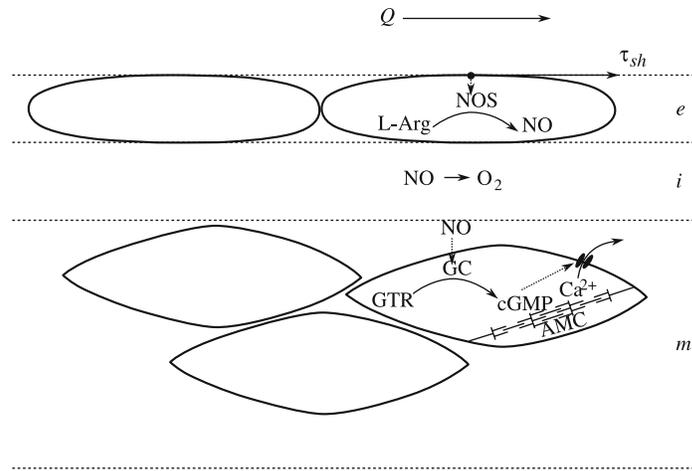
Fig. 1. Diagram of the autoregulation process related with the shear stress and the diffusion-kinetic processes in the endothelial cells (e) and the intima (i) and media (m) layers: NOS is NO production catalyst, L-Arg is L-arginine, GC is cGMP production catalyst, GTP is guanosine-triphosphate, cGMP is cyclic guanosine-monophosphate, AMC is actin-myosin complex.

muscular-tissue relaxation also made it possible to understand the operating principle of the emergency preparation nitroglycerine previously used without its role being completely understood.

The mechanical nature of the regulation of the muscular tonus of the arterial wall was discussed in [7, 16–19]. It was shown that an increase in the shear stress between the blood flow and the inner arterial surface leads to the relaxation of the smooth muscle layer in the arterial wall. This is followed by an increase in the artery radius and a decrease in the shear stress; therefore, the entire process is characterized by the presence of feedback.

In the arterial wall three main layers can be distinguished. The first, inner, layer or intima (i), the middle layer or media (m), and the outer layer or adventitia (a). The inner surface of the i-layer is lined with endothelial cells. The m-layer contains many smooth muscle cells. The layer thicknesses depend on the type of artery or arteriole. In what follows we will consider resistive arteries with a developed muscular layer in m and a non-negligibly thin i-layer. The typical intima to media thickness ratio is of the order of 10^{-1}.

The scenario of the effect of a change in the vessel wall shear stress on the vessel muscle relaxation is as follows. An increase in the shear stress τ_{sh} on the surface of the endothelial cells opens the calcium channels, which leads to an increase in nitric oxide (NO) synthesis from L-arginine catalyzed by NO-synthase. Nitric oxide then diffuses with absorption across the intima layer to the smooth muscle cells in the m-layer. Being a lipophilic molecule, NO easily penetrates the membranes of the smooth muscle cells and initiates the synthesis of cyclic guanosine monophosphate. The latter stimulates the outflow of intracellular calcium ions (Ca^{2+}), which reduces the concentration of the contracting actin-myosin complexes and hence leads to the relaxation of the smooth muscle cells. The flow-dependent vessel constriction follows a similar course. A diagram of the autoregulation process is shown in Fig. 1.

The arterial wall has one more property that distinguishes it from an ordinary elastic tube: this is its viscoelasticity, which is needed for its damping function, that is, for smoothing the pressure waves, and which makes a significant contribution to the artery's behavior [20, 21].

The purpose of our study is to formulate and investigate a novel mathematical model for describing the local autoregulation of the blood flow with account for the viscoelastic behavior of the arterial wall and those two-layer diffusion and kinetic processes in which the concentrations of the key agents: nitric oxide (NO), calcium ions (Ca^{2+}), and phosphorylated myosin, are involved.

1. MAIN ASSUMPTIONS OF THE MODEL

We will consider an axially symmetric and viscoelastic artery. We assume the blood to be an incompressible and viscous fluid, the flow quasi-stationary, and the transmural pressure P_0 (difference of the pressures acting on the vessel wall) constant. For the radial profile of the axial velocity a power generalization of the Poiseuille law is used. A linear dependence of the muscular force on the phosphorylated myosin concentration in the smooth muscle cell is assumed. The rate of NO production in the endothelial layer on the inner surface of the arterial wall is assumed to be proportional to the shear stress.

2. FORMULATION OF THE PROBLEM

Let us consider an artery segment of length l with cross-sectional area A and wall thickness h in the cylindrical coordinate system $(r, \theta, x \equiv z)$. The intima, media and adventitia layers have the coordinates R_i, R_m, and R_a, respectively.

1. *Dependence of the shear stress on the blood flow-rate.* Let the velocity profile have the form [3]:

$$V_x(r, x, t) = \frac{s + 2}{s}\left[1 - \left(\frac{r}{R(t)}\right)^s\right]u(x, t). \tag{2.1}$$

Here, V_x is the axial flow velocity component, u is the axial velocity component averaged over the cross-section, R is the inside radius of the artery, and s is the steepness of the velocity profile. The case $s = 2$ corresponds to the parabolic velocity profile describing laminar Newtonian fluid flow along a rigid cylindrical tube.

In the case of a fluid with the dynamic viscosity μ in the boundary layer the shear stress on the tube wall can be expressed by the formula

$$\tau_{sh} = -\mu\left[\frac{\partial V_x}{\partial r}\right]_{r=R} = (s + 2)\mu\frac{u}{R} = (s + 2)\mu\frac{Q}{\pi R^3}, \tag{2.2}$$

where $Q = Au$ is the blood volume flow-rate through a cross-section of area A.

Taking into account (2.1) and (2.2) and averaging the fluid mass and momentum conservation equations over the cross-section, we obtain

$$\frac{\partial A}{\partial t} + \frac{\partial Q}{\partial x} = 0, \tag{2.3}$$

$$\frac{\partial Q}{\partial t} + \frac{\partial}{\partial x}\left(\alpha_0\frac{Q^2}{A}\right) + \frac{A}{\rho}\frac{\partial P}{\partial x} = -2\pi\nu(s + 2)\frac{Q}{A}, \tag{2.4}$$

where $\alpha_0 = (s + 2)/(s + 1)$ is a correcting multiplier for the momentum [3] for the given velocity profile (2.1).

Assuming that a quasi-stationary laminar flow is realized, we can reduce the system (2.3), (2.4) to the generalized Hagen–Poiseuille equation [22]

$$\frac{\partial Q}{\partial x} = 0, \qquad Q = \frac{\pi R^4}{2(s + 2)\mu}\frac{\Delta P}{l}, \tag{2.5}$$

where ΔP is the pressure difference on the artery segment of length l.

Following [22], we will assume that the change in the blood flow-rate due to the motion of the arterial wall is inconsiderable and that the viscous forces predominate over the inertial ones (the Reynolds number is small). Thus, the blood flow-rate level is determined by the pressure gradient.

From Eqs. (2.5) it can be seen that the blood flow-rate linearly depends on the pressure gradient and is proportional to the fourth power of the artery radius.

We will consider the process of local autoregulation on an artery segment sufficiently short for the quasi-stationary pressure, flow-rate and radius to be constant over the entire segment.

For axially-symmetric radial perturbations $R(t) = R_0(1 + \eta(t))$, from (2.2) we obtain

$$\tau_{sh} = \frac{(s + 2)\mu}{\pi R_0^3} \frac{Q}{(1 + \eta)^3}. \tag{2.6}$$

There is a hypothesis to the effect that a constant shear stress value tends to be maintained: $\tau_{sh} = \text{const}$ [7, 23]. An increase in flow-rate leads to an increase in the equilibrium artery radius in order to compensate the increase in the shear stress. From (2.6) there follows the estimate for the relationship between the new steady blood flow-rate and the new stationary value of the artery radius

$$\frac{R - R_0}{R_0} = \left(\sqrt[3]{\frac{Q}{Q_0}} - 1 \right). \tag{2.7}$$

We note a difference in the artery response to an increase and decrease in the blood flow-rate near the previous stationary value. The change in the radius in response to an increase in the flow-rate is smaller than that in response to a decrease of the same magnitude. This must be attributable to the inverse cubic dependence of the shear stress on the artery radius.

For small radial perturbations ($|\eta| \ll 1$) the artery radius perturbation depends almost linearly on the blood flow-rate.

2. *Synthesis and diffusion of nitric oxide.* In accordance with the endothelium-dependent mechanism which controls the blood flow, the concentration of the nitric oxide produced by the endothelial cell is determined by the shear stress (Fig. 1).

We will regard the transport of NO to the smooth muscle tissue as a diffusion process with absorption (D_1 is the diffusion coefficient and δ_1 is the reaction rate). In the smooth muscle tissue nitric oxide continues to diffuse with the diffusion coefficient D_2 and the reaction rate δ_2.

In the endothelium nitric oxide production is determined by the shear stress τ_{sh}. Therefore, this process can be described by the kinetic equation

$$\frac{dn_e}{dt} = -k_e n_e + k_3 \tau_{sh}(t), \tag{2.8}$$

where n_e is the NO concentration in the endothelial cell, k_e is a coefficient characterizing nitric oxide mass transfer from the cell into the blood flow, and k_3 is a production constant.

As an inner boundary condition for nitric oxide diffusion across the arterial wall the solution of Eq. (2.8) $[n]_{r=R_i} = n_e$ is used. On the interface between the i- and m-layers the equality of the concentrations and diffusion fluxes is taken into account. On the outer boundary of the m-layer the impermeability condition is assigned.

Thus, with account for (2.6) and (2.8), the system of equations and boundary conditions for the nitric oxide concentration has the form:

$$\frac{dn_e}{dt} = -k_e n_e + \frac{\psi_0}{(1 + \eta(t))^3},$$

$$\frac{\partial n_j}{\partial t} = D_j \frac{1}{r} \frac{\partial}{\partial r} \left(r \frac{\partial n_j}{\partial r} \right) - \delta_j n_j,$$

$$R_i < r < R_m, \quad j = 1 \ (i), \qquad R_m < r < R_a, \quad j = 2 \ (m), \tag{2.9}$$

$$[n_1]_{r=R_i} = n_e, \qquad [n_1]_{r=R_m} = [n_2]_{r=R_m},$$

$$\left[D_1 \frac{\partial n_1}{\partial r} \right]_{r=R_m} = \left[D_2 \frac{\partial n_2}{\partial r} \right]_{r=R_m}, \qquad \left[\frac{\partial n_2}{\partial r} \right]_{r=R_a} = 0.$$

Here, $\psi_0 = k_3(s + 2)\mu Q/\pi R_0^3$ and R_i, R_m, and R_a are the coordinates of the i-, m- and a- layer boundaries, respectively.

In (2.9) it is assumed that for NO a first-order reaction occurs. System of equations (2.9), together with the initial conditions, describes the two-layer diffusion-kinetic process for nitric oxide in the arterial wall.

3. *Equation for the kinetics of the calcium ions in the smooth muscle cell.* In deriving the balance equation for the Ca^{2+} concentration in the smooth muscle cell we will take into account the inward and outward calcium fluxes. There are two sources of calcium ions: the extracellular space and the intracellular containers, sarcoplasmic reticulum, where the Ca^{2+} concentration is 10^4 times higher than in the intracellular space. The balance of calcium ions in the smooth muscle cell layer corresponding to a coordinate r can be described by the relation

$$\frac{\partial C(r, t)}{\partial t} = -\alpha(n)C + \beta(P)(C_e - C), \tag{2.10}$$

where the first term is responsible for the active transport of Ca^{2+} from the intracellular space and the second describes the passive transport of calcium ions through calcium channels, which is determined by the difference between the extracellular C and intracellular C_e concentrations.

Generally, the active transport coefficient $\alpha(n)$ depends on the NO concentration in the smooth muscle cell, whereas the transmission coefficient $\beta(P)$ is a function of the blood pressure [17]. Assuming that the dependence of α on the NO concentration is linear and taking into account that, by virtue of the assumption of constancy of the transmural pressure, $\beta = \mathrm{const}$, we have

$$\alpha(n) = \alpha_1 + k_1 n_2(r, t), \qquad \alpha_1, k_1 = \mathrm{const}, \tag{2.11}$$

where α_1 is a coefficient corresponding to the NO-independent active Ca^{2+} evacuation and k_1 is a coefficient characterizing the NO-mediated decrease in the intracellular calcium ion concentration.

Taking into account that $C_e \gg C$, we will treat the second term on the right side of (2.10) as a constant source φ_0. Equation (2.10) then takes the form:

$$\frac{\partial C}{\partial t} = -\alpha_1 C - k_1 n_2 C + \varphi_0. \tag{2.12}$$

Here, $\varphi_0 = \beta C_e = \mathrm{const}$. Equation (2.12) is used for describing the calcium ion kinetics in the smooth muscle layer.

4. *Kinetics equation for active myosin which determines the muscular tonus.* The stress developed by the smooth muscle cell as a result of contraction is determined by the activity level of the myosin heads, which, in its turn, depends on the intracellular concentration of calcium ions and on the Ca^{2+} sensitivity threshold of the specific myosin-activating (phosphorylating) ferments.

We will describe the phosphorylated myosin kinetics in the same way as the calcium ion kinetics:

$$\frac{\partial f(r, t)}{\partial t} = -\alpha_2 f + \gamma(C - C_{th})\theta(C - C_{th}), \tag{2.13}$$

where the first term is responsible for the process of myosin dephosphorylation (deactivation) and the second describes the calcium-dependent activation of the actin-myosin complex with account for the threshold of sensitivity to the Ca^{2+} concentration. Here, θ is the Heaviside unit function, α_2 and γ are the phosphorylation and dephosphorylation rate coefficients, and C_{th} is the threshold concentration (in general, presumed to depend on the NO concentration). In what follows we will assume the parameters of Eq. (2.13) to be constant.

Equation (2.13) will be used for describing the regulation of the muscular stress by calcium ions.

5. *Equation of motion of the arterial wall.* In order to construct a closed system of blood flow autoregulation, it is necessary to have the relationship between the artery radius perturbation and external forces such as the pressure and the muscular force [24]. The corresponding equation of motion for a segment of the arterial wall can be obtained with account for the constitutive equation for the arterial wall tissue [21, 25].

We will consider a viscoelastic wall element of mass Δm, density ρ_w, thickness h, radius R, and length Δx. According to the momentum conservation law,

$$\Delta m \frac{d^2 R}{dt^2} = f_r + f_p,$$

$$f_r = -\sigma_{\theta\theta} 2\pi h \Delta x, \qquad f_p = (P - P_e) 2\pi R \Delta x,$$

(2.14)

where $\Delta m = \rho_w 2\pi R \Delta x h$, f_r is proportional to the tangential stress tensor component $\sigma_{\theta\theta}$, and f_p is the resulting transmural pressure (the difference $P_0 = P - P_e$ between the internal and external pressures).

The stress tensor component $\sigma_{\theta\theta}$ consists of three terms: the passive elastic force (weakly nonlinear with a quadratic correction), the viscous resistance force, and the active force due to muscular tonus:

$$\sigma_{\theta\theta} = \frac{E(F)}{1 - \xi^2}\left[\frac{R - R_0}{R_0} + \kappa_1\left(\frac{R - R_0}{R_0}\right)^2\right] + \lambda\frac{dR}{dt} + k_2 F.$$

(2.15)

Here, $E(F)$ is Young's modulus, which depends on the volume-averaged phosphorylated myosin concentration in the muscular layer, ξ is Poisson's ratio, κ_1 and λ are the nonlinear-elasticity and viscosity coefficients of the arterial wall, $F = \langle f(r, t) \rangle$ is the concentration of contracting actin-myosin filaments averaged over the smooth muscle layer volume, which determines the active muscular stress, and k_2 is the coefficient of proportionality of the muscular tonus response to the phosphorylated myosin concentration.

Substituting (2.15) in (2.14) with account for the linear dependence of the muscular force on the myosin concentration, for $h_0 R_0 = hR$ we obtain the equation for the radius perturbation η $(R = R_0(1 + \eta), |\eta| \ll 1)$

$$\rho_w h_0 R_0 \frac{d^2 \eta}{dt^2} + \lambda h_0 \frac{d\eta}{dt} + \kappa(F)[\eta + \kappa_1 \eta^2] = (P - P_e) - \frac{h_0}{R_0} k_2 F,$$

(2.16)

$$\kappa(F) = \kappa_0\left(1 + \varepsilon\frac{F}{F_0}\right), \quad \kappa_0 = \frac{h_0 E_0}{R_0(1 - \xi^2)}, \quad F = \frac{2}{R_a^2 - R_m^2}\int_{R_m}^{R_a} f(r, t)\, r\, dr,$$

(2.17)

where F_0 is the volume-averaged concentration of the stationary active myosin distribution $f^{(0)}(r)$.

We thus obtain the integro-differential equation for describing the wall motion with account for muscular tonus

$$\rho_w h_0 R_0 \frac{d^2 \eta}{dt^2} + \lambda h_0 \frac{d\eta}{dt} + \kappa(F)[\eta + \kappa_1 \eta^2] = P_0 - \frac{h_0 k_2}{R_0} F.$$

(2.18)

In the absence of muscular forces (complete relaxation of the wall), from Eq. (2.18) we obtain the equation of a nonlinear damped oscillator with an external driving force P_0. The dependence on the myosin concentrations provides feedback and differentiates the artery from a passive viscoelastic tube.

6. *Formulation of the problem of blood flow autoregulation in dimensionless variables.* The system of equations for describing the autoregulation process has the form:

$$\frac{dn_e}{dt} = -k_e n_e + \frac{\psi_0}{(1 + \eta)^3},$$

(2.19)

$$\frac{\partial n_i}{\partial t} = D_i \frac{1}{r}\frac{\partial}{\partial r}\left(r\frac{\partial n_i}{\partial r}\right) - \delta_i n_i,$$

$$i = 1: \quad R_i < r < R_m, \qquad i = 2: \quad R_m < r < R_a,$$

(2.20)

$$\frac{\partial C(r,\,t)}{\partial t} = -\alpha_1 C - k_1 n_2(r,\,t)C + \varphi_0, \qquad R_m < r < R_a, \tag{2.21}$$

$$\frac{\partial f(r,\,t)}{\partial t} = -\alpha_2 f + \gamma[C - C_{th}]\theta(C - C_{th}), \qquad R_m < r < R_a, \tag{2.22}$$

$$\rho_w h_0 R_0 \frac{d^2\eta}{dt^2} + \lambda h_0 \frac{d\eta}{dt} + \kappa(F)[\eta + \kappa_1 \eta^2] = P_0 - \frac{h_0 k_2}{R_0} F. \tag{2.23}$$

We will use the boundary conditions

$$[n_1]_{r=R_i} = n_e, \qquad [n_1]_{r=R_m} = [n_2]_{r=R_m},$$

$$\left[D_1 \frac{\partial n_1}{\partial r}\right]_{r=R_m} = \left[D_2 \frac{\partial n_2}{\partial r}\right]_{r=R_m}, \qquad \left[\frac{\partial n_2}{\partial r}\right]_{r=R_a} = 0. \tag{2.24}$$

As initial conditions we will take functions similar to the stationary solutions.

Equation (2.19) describes the synthesis of nitric oxide in the endothelial cell, which depends on the shear stress value, Eq. (2.20) characterizes the NO diffusion in the i- and m-layers, respectively, Eq. (2.21) describes the Ca^{2+} balance in the smooth muscle cell, Eq. (2.22) corresponds to the generation of the active muscular stress (via the concentration of contracting actin-myosin complexes) determined by the calcium ion concentration level, and Eq. (2.23) determines the arterial wall motion under the effect of the average active myosin concentration.

In the system of equations (2.19)–(2.24) we introduce the dimensionless variables

$$n_e = n^0 n_e', \qquad n_1 = n^0 n_1', \qquad n_2 = n^0 n_2',$$

$$C = C_{th} C', \qquad f = f^0 f', \qquad \eta = \eta' = \frac{R - R_0}{R_0}, \tag{2.25}$$

$$t = t_0 t', \qquad r = R_0 r',$$

$$n^0 = n_e^0 \equiv \frac{\psi_0}{k_e} = \frac{k_3(s+2)\mu Q}{k_e \pi R_0^3}, \tag{2.26}$$

$$f^0 \equiv F_0 = \frac{2}{R_a^2 - R_m^2} \int_{R_m}^{R_a} f^{(0)}(r)r\,dr.$$

After substituting (2.25) we obtain the system of equations (2.21)–(2.23) in the form (we omit the primes on the variables):

$$\frac{dn_e}{dt} = -k_e' n_e + \frac{\psi_0'}{(1+\eta)^3},$$

$$\frac{\partial n_i}{\partial t} = D_i' \frac{1}{r} \frac{\partial}{\partial r}\left(r \frac{\partial n_i}{\partial r}\right) - \delta_i' n_i,$$

$$i = 1: \quad 1 < r < R_m', \qquad i = 2: \quad R_m' < r < R_a' \tag{2.27}$$

$$\frac{\partial C}{\partial t} = -\alpha_1' C - k_1' n_2 C + \varphi_0', \qquad R_m' < r < R_a',$$

$$\frac{\partial f}{\partial t} = -\alpha_2' f + \gamma'[C - 1]\theta(C - 1), \qquad R_m' < r < R_a',$$

$$\frac{d^2\eta}{dt^2} + \lambda' \frac{d\eta}{dt} + \kappa_0'(1 + \varepsilon F)[\eta + \kappa_1 \eta^2] = P_0' - k_2' F, \quad F = \frac{2}{R_a'^2 - R_m'^2} \int_{R_m'}^{R_a'} fr\,dr,$$

$$k'_e = k_e t_0, \qquad \psi'_0 = \frac{\psi_0 t_0}{n^0}, \qquad D'_{1,2} = \frac{D_{1,2} t_0}{R_0^2}, \qquad \delta'_{1,2} = \delta_{1,2} t_0,$$

$$\alpha'_{1,2} = \alpha_{1,2} t_0, \qquad k'_1 = k_1 n^0 t_0, \qquad \varphi'_0 = \frac{\varphi_0 t_0}{C_{th}}, \qquad \gamma = \frac{\gamma C_{th} t_0}{f^0}, \tag{2.28}$$

$$\lambda' = \frac{\lambda t_0}{\rho_w R_0}, \qquad \kappa'_0 = \frac{\kappa_0 t_0^2}{\rho_w h_0 R_0} \equiv \frac{E_0 t_0^2}{\rho_w R_0^2 (1 - \xi^2)},$$

$$P'_0 = \frac{P_0 t_0^2}{\rho_w h_0 R_0}, \qquad k'_2 = \frac{k_2 f^0 t_0^2}{\rho_w R_0^2}.$$

The boundary conditions are used in form (2.24) for $r = 1$, $r = R'_m$, and $r = R'_a$, where $R_0 = R_i$, $R'_m = R_m/R_0$, and $R'_a = R_a/R_0$. The initial conditions are taken close to the stationary solutions of system (2.27).

From the first of equations (2.27), with account for (2.26) and (2.28), there follows the dependence of the nitric oxide concentration in the endothelium on the blood flow-rate Q, since the coefficient $\psi'_0 \sim n^0 \sim Q$.

3. STATIONARY SOLUTION OF THE AUTOREGULATION PROBLEM

We will consider stationary solutions of the problem, setting

$$n_e = 1, \quad n_{1,2} = n_{1,2}^{(0)}(r), \quad C = C^{(0)}(r), \quad f = f^{(0)}(r), \quad \eta = 0. \tag{3.1}$$

In this case, for describing the local autoregulation process we can rewrite the system of equations (2.27) in the form:

$$\frac{d^2 n_i^{(0)}}{dr^2} + \frac{1}{r} \frac{dn_i^{(0)}}{dr} - \frac{\delta'_i}{D'_i} n_i^{(0)} = 0,$$

$$i = 1: \; 1 \le r \le R'_m, \qquad i = 2: \; R'_m \le r \le R'_a,$$

$$C^{(0)}(r) = \frac{\varphi'_0}{\alpha'_1 + k'_1 n_2^{(0)}(r)}, \quad R'_m \le r \le R'_a, \tag{3.2}$$

$$f^{(0)}(r) = \frac{\gamma'}{\alpha'_2} [C^{(0)}(r) - 1] \theta(C^{(0)}(r) - 1), \quad R'_m \le r \le R'_a,$$

$$P'_0 = \frac{2k'_2}{R'^2_a - R'^2_m} \int\limits_{R'_m}^{R'_a} f^{(0)}(r) \, r \, dr$$

with the boundary conditions

$$\left[n_1^{(0)} \right]_{r=1} = 1, \quad \left[n_1^{(0)} \right]_{r=R'_m} = \left[n_2^{(0)} \right]_{r=R'_m},$$

$$D_1 \left[\frac{dn_1^{(0)}}{dr} \right]_{r=R'_m} = D_2 \left[\frac{dn_2^{(0)}}{dr} \right]_{r=R'_m}, \quad \left[\frac{dn_2^{(0)}}{dr} \right]_{r=R'_a} = 0. \tag{3.3}$$

The ordinary differential equations (3.2) for the NO concentration have general solutions which can be expressed in terms of the modified Bessel functions $I_0(z)$ and $K_0(z)$

$$n_1^{(0)}(r) = A_1 I_0 \left(\sqrt{\frac{\delta'_1}{D'_1}} r \right) + A_2 K_0 \left(\sqrt{\frac{\delta'_1}{D'_1}} r \right),$$

$$n_2^{(0)}(r) = B_1 I_0 \left(\sqrt{\frac{\delta'_2}{D'_2}} r \right) + B_2 K_0 \left(\sqrt{\frac{\delta'_2}{D'_2}} r \right), \tag{3.4}$$
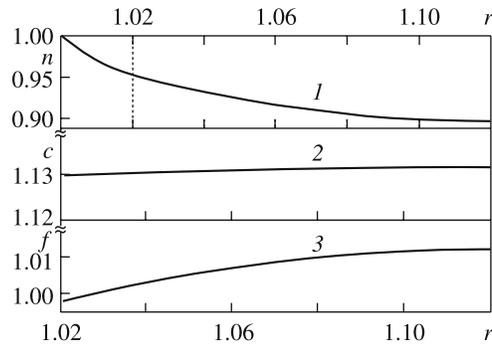
Fig. 2. Stationary concentration distributions in the arterial wall: NO (*1*), intracellular Ca^{2+} (*2*), phosphorylated myosin (*3*).

where A_1, A_2, B_1, and B_2 are arbitrary constants which can be found from boundary conditions (3.3):

$$A_1 I_0(\xi_1) + A_2 K_0(\xi_1) = 1, \quad B_1 I_1(\xi_2 R'_a) - B_2 K_1(\xi_2 R'_a) = 0,$$

$$A_1 I_0(\xi_1 R'_m) + A_2 K_0(\xi_1 R'_m) = B_1 I_0(\xi_2 R'_m) + B_2 K_0(\xi_2 R'_m),$$

$$D_1 \xi_1 (A_1 I_1(\xi_1 R'_m) - A_2 K_1(\xi_1 R'_m)) = D_2 \xi_2 (B_1 I_1(\xi_2 R'_m) - B_2 K_1(\xi_2 R'_m)), \qquad (3.5)$$

$$\xi_1 \equiv \sqrt{\delta'_1/D'_1}, \qquad \xi_2 \equiv \sqrt{\delta'_2/D'_2}.$$

Using the experimental data [22, 26, 27] for resistive muscular arteries (see the table), we find the constants A_1, A_2, B_1, and B_2 from boundary conditions (3.5).

The stationary concentrations of calcium ions $C^{(0)}(r)$ and phosphorylated myosin $f^{(0)}(r)$ in the smooth muscle layer can be determined from the corresponding equations. The equilibrium distributions of the NO, Ca^{2+} and myosin concentrations are shown in Fig. 2 (the broken line is the interface between the *i*- and *m*-layers).

4. CASE OF A THIN-WALLED ARTERY

In order to understand the system behavior qualitatively, we will consider the limiting case of a thin-walled artery. A similar model was studied by A. Rachev and S.A. Regirer [7, 9]. We will first obtain estimates that make it possible to go over to this limiting case. The first inequality $h_i/h_m \ll 1$ enables us to consider only one layer for the diffusion-kinetic processes. The second is $T_{dif} \ll T_{kin}$, where $T_{dif} = h^2/D$ and $T_{kin} = \min\{1/\delta, n_0/\psi_0, \dots\}$ are the characteristic times of the diffusion and kinetic processes. Here, h_i and h_m are the thicknesses of the *i*- and *m*-layers, respectively, and h is the spatial scale of the wall thickness. Assuming that for nitric oxide the kinetic processes occur more rapidly in the vessel wall than on the inner boundary (in the endothelium) we have

$$h \ll \sqrt{\frac{D}{\delta}} \equiv h_0, \qquad (4.1)$$

where h_0 is a characteristic wall thickness for which passage to the limit is possible and δ is the kinetic mass-transfer coefficient. Taking into account that typical values of the parameters are $D = 3300 \ \mu m^2/s$ and $\delta = 0.25 \ s^{-1}$ [12, 22], we obtain $h_0 \simeq 115 \ \mu m$.

For arteries of large and medium diameter the characteristic h value varies from 100 to 1000 μm, whereas for small arteries and arterioles the thicknesses are smaller: $h \sim 10 \ \mu m$. Thus, the limiting case considered describes the blood flow autoregulation in small arteries with $h \ll 100 \ \mu m$.

In this case, the intima and media layers are sufficiently thin for it to be possible to disregard the multilayer structure of the arterial wall and diffusion in it.

Table

Parameter	Value	Source
R_0	2000 μm	[30]
h_0	450 μm	[30]
ψ_0	0.1 μmol/s	[12]
α_1	0.05 s^{-1}	[7]
α_2	0.5 s^{-1}	[17]
$D_{1,2}$	3300 μm^2/s	[22]
δ_1	0.1 s^{-1}	[22]
δ_2	0.01 s^{-1}	[22]
E	3×10^5 Pa	[3]
ρ_w	1100 kg/m^3	[3]
P_0	115 mm Hg	[30]
Q_0	105 ml/min	[30]

If we average over the thickness of the wall and neglect its inertia (since the natural wall oscillation period is small as compared with the characteristic times of the kinetic processes), system (2.27) takes the form:

$$\frac{dn}{dt} = -kn + \frac{a}{(1 + y)^3},$$

$$\frac{dx}{dt} = -\alpha_1 x - k_1 nx - \gamma_1 n + b,$$

$$\frac{df}{dt} = -\alpha_2 f + \gamma_2 x,$$

$$\frac{dy}{dt} = -\frac{A}{\beta} - \frac{\kappa_0}{\beta}(1 + \varepsilon f)[y + \kappa_1 y^2] + \frac{B}{\beta},$$

(4.2)

where $n \equiv n_e(t)/n_0$ and $x \equiv (C(t) - C_{th})/x_0$ are concentrations of nitric oxide in the endothelium and of Ca^{2+} in the smooth muscle layer higher than the threshold concentration, $f = f(t)/f_0$ is the concentration of active myosin in the smooth muscle cells (n_0, x_0, and f_0 are characteristic concentrations), $y \equiv \eta(t) = (R - R_0)/R_0$ is the vessel radius deviation ($|\eta| \ll 1$), and the dimensionless constants are determined by the formulas $k = k'_e$, $a = \psi'_0$, $\alpha_{1,2} = \alpha'_{1,2}$, $k_1 = k'_1$, $\gamma_1 = k'_1 C_{th}/x_0$, $b = (\varphi'_0 - \alpha'_1)C_{th}/x_0$, $\gamma_2 = \gamma' x_0/C_{th}$, $\beta = \lambda'$, $\kappa_0 = \kappa'_0$, $A = k'_2$, and $B = P'_0$ (see (2.28)).

We will find the stationary points of system (4.2). Taking into account that

$$\frac{bk - a\gamma_1}{\alpha_1 k + ak_1} = \frac{\alpha_2 B}{\gamma_2 A},$$

(4.3)

we obtain the stationary point $\{n = a/k, x = \alpha_2 B/\gamma_2 A, f = B/A, y = 0\}$ corresponding to the undisturbed artery state. Relation (4.3) reflects the balance between the muscular forces determined by the calcium ion concentration and the blood pressure forces. The equilibrium Ca^{2+} concentration is equal to $\alpha_2 B/\gamma_2 A \sim P_0 R_0/f_0 h_0$.

We will investigate the stability of the dynamic system (4.2) on the assumption that the myosin phosphorylation process is quasi-stationary ($f = \gamma_2 x/\alpha_2$). We will consider the linearized system near the stationary point of the simplified system $\{n_0 = a/k, x_0 = B/A_1, y_0 = 0\}$, taking into account the relation
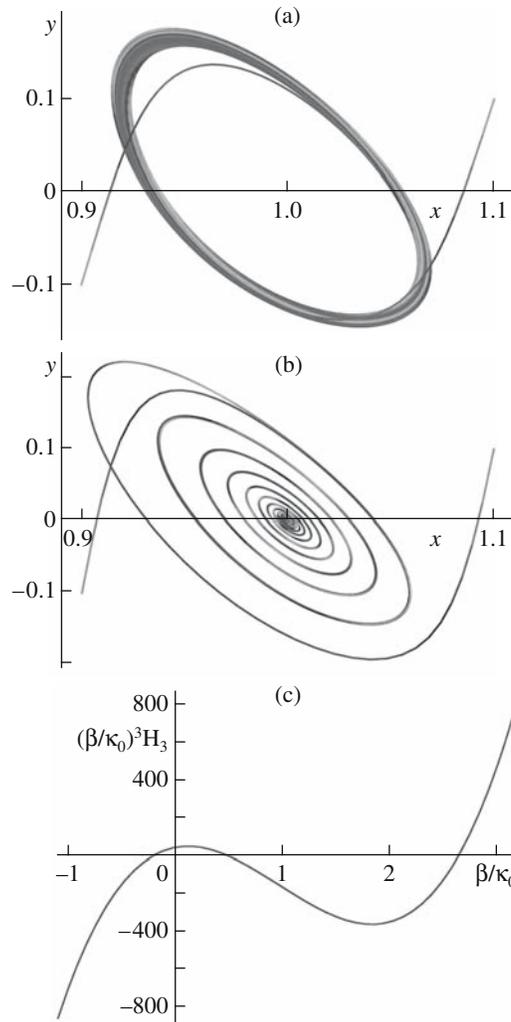
Fig. 3. Phase trajectory of system (4.2) in the plane (x, y) for different values of the wall viscosity parameter (a), (b) and regions of linear stability of the dynamic system in the parameter β, corresponding to the upper half-plane (c).

$$\frac{d\mathbf{X}}{dt} = M\mathbf{X} + \mathbf{F}, \tag{4.4}$$

$$M = \begin{pmatrix} -k & 0 & -3a \\ -C & -D & 0 \\ 0 & -\dfrac{A_1}{\beta} & -\dfrac{\kappa}{\beta} \end{pmatrix}, \quad \mathbf{X} = (n, x, y)^{\mathrm{T}}, \quad \mathbf{F} = \left(a, \; b + k_1 n_0 x_0, \; \frac{B}{\beta} \right)^{\mathrm{T}},$$

$$A_1 = \frac{\gamma_2 A}{\alpha_2}, \quad \varepsilon_1 = \frac{\gamma_2 \varepsilon}{\alpha_2}, \quad C = k_1 x_0 + \gamma_1, \quad D = k_1 n_0 + \alpha_1, \quad \kappa = \kappa_0 (1 + \varepsilon_1 x_0).$$

The Routh–Hurwitz criterion yields a condition for the Hurwitz determinants, composed of the coefficients of the characteristic polynomial of the matrix M, which ensures the negativeness of the real parts of all the eigenvalues of this matrix. The stability condition is

$$(kD^2 + k^2 D)\beta^2 + (\kappa D^2 + 2k\kappa D - 3aA_1 C + k^2 \kappa)\beta + \kappa^2 D + k\kappa^2 > 0. \tag{4.5}$$

Relation (4.5) makes it possible to determine the range of the arterial-wall viscosity β values on which the equilibrium state is linearly stable.

The results of a numerical stability analysis for the initial system (4.2) are shown in Fig. 3. Taking into account that the coefficients of system (4.2) are positive, a sufficient condition of linear stability in the parameter β is obtained (the upper half-plane in Fig. 3a corresponding to a positive determinant H_3).

For the region of nonlinear stability in the wall viscosity parameter (the lower half-plane in Fig. 3c) it is shown that a regime of undamped periodic oscillations exists. This suggests that, for the endothelium-dependent blood flow regulation factor to function normally in the vessel and for this factor to interact with the other regulatory mechanisms, the viscosity parameter β must lie within the range of undamped oscillations. The role of the model dissipation in providing stability within the framework of the endothelium-dependent mechanism was noted in [9].

A numerical analysis in the phase space (n, x, f, y) confirms the preliminary estimates (see the two-dimensional projection of the system phase trajectory on the plane (x, y), Fig. 3): if β lies outside the range of linear stability, a limit cycle develops (a) and if it lies within this range, damped oscillations (b) can be observed.

5. CASE OF A PASSIVE VESSEL

From the limiting case of a thin-walled artery it can be seen that the higher the blood flow-rate at a constant transmural pressure, the lower the equilibrium calcium concentration. In the initial model a variable distribution of the Ca^{2+} concentration in the vessel wall is realized. With decrease in the equilibrium calcium concentration over the entire wall thickness to a level lower than the threshold level C_{th} the muscular layer completely relaxes. In this case, the "active" viscoelastic tube becomes "passive". In dimensionless form the equation of motion for the arterial wall is as follows:

$$\frac{d^2\eta}{dt^2} + \lambda \frac{d\eta}{dt} + \kappa_0(\eta + \kappa_1\eta^2) = P_0. \tag{5.1}$$

We will obtain an exact solution of Eq. (5.1) using the method of "simplest equations" [28] which generalizes certain existing approaches, such as the "hyperbolic tangent" and "elliptic test function" methods [29].

Taking into account the second-order pole in the general solution of (5.1), we will seek a solution in the form of expansion

$$\eta(t) = A_0 + A_1 G(t) + A_2 G(t)^2, \tag{5.2}$$

where $G(t)$ is a solution, with first-order pole, of the equation

$$\frac{dG(t)}{dt} = kG(t) - kG(t)^2. \tag{5.3}$$

Here, A_0, A_1, A_2, and k are arbitrary constants to be found.

Substituting expansion (5.2) in Eq. (5.1), we find

$$A_0 = -\frac{30\lambda k + 25\kappa_0 - \lambda^2 + 25k^2}{50\kappa_0\kappa_1}, \qquad A_1 = \frac{6k(\lambda + 5k)}{5\kappa_0\kappa_1},$$

$$A_2 = -\frac{6k^2}{\kappa_0\kappa_1}, \qquad P_0 = -\frac{-36\lambda^4 + 625\kappa_0^2}{2500\kappa_0\kappa_1}, \qquad k = \pm\frac{\lambda}{5}. \tag{5.4}$$

Using the solution $G(t) = 0.5[1 + \tanh(0.5k(t - t_0))]$ of the auxiliary equation (5.3) and taking $k = \lambda/5$, we obtain an exact solution of Eq. (5.1) in the form:

$$\eta(t) = \frac{1}{50\kappa_0\kappa_1}(3\lambda^2 - 25\kappa_0 + 6\lambda^2\tanh[0.1\lambda(t - t_0)] - 3\lambda^2\tanh^2[0.1\lambda(t - t_0)]), \tag{5.5}$$

where t_0 is an arbitrary constant.
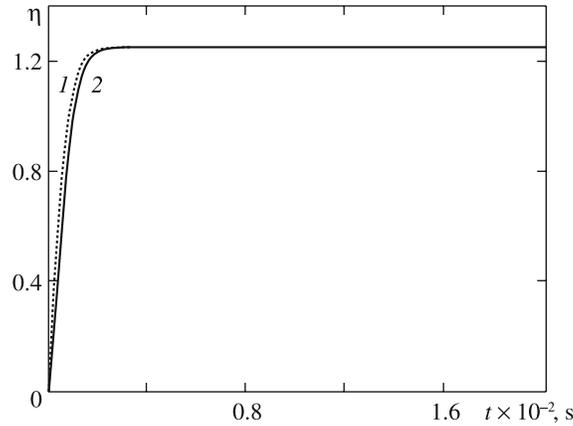
Fig. 4. Comparison of the exact (*1*) and numerical (*2*) solutions of Eq. (5.1) describing the passive dilatation of the artery.

Given the additional condition $\eta(0) = 0$, $t_0 = 0$ the following relationships between the parameters hold:

$$\kappa_0 = \frac{4\kappa_1 P_0}{3}, \quad \lambda = \sqrt{\frac{25\kappa_0}{3}}. \tag{5.6}$$

Having simplified (5.5), with account for (5.6) we finally obtain the solution of Eq. (5.1) in the form of a kink, which describes the passive dilatation of the artery:

$$\eta(t) = \eta_\infty \tanh\left(\frac{\lambda t}{10}\right)\left(2 - \tanh\left(\frac{\lambda t}{10}\right)\right), \quad \eta_\infty = \frac{2P_0}{3\kappa_0}. \tag{5.7}$$

Solution (5.7) represented by curve *1* in Fig. 4 is a switching wave which characterizes the transition of the system from one stationary state to another under the action of a constant force field.

We note that solution (5.7) describes the undisturbed state of the artery at the initial moment $\eta(0) = 0$, when the pressure and the smooth muscular force equilibrate each other. After the muscular force has disappeared (due to a sharp decrease in the calcium level), the artery dilates until a balance between the blood pressure and wall elasticity forces is reached, that is, goes over into a new equilibrium state.

The new artery radius, which depends on the pressure P_0 and the elastic properties of the wall, can be estimated as η_∞.

6. NUMERICAL INVESTIGATION OF THE AUTOREGULATION PROBLEM

For describing the blood flow regulation process in the general case, the two-layer diffusion-kinetic model (2.27) was considered. The problem was solved numerically using an implicit finite difference method. In each time step, to find the radius deviation, we carried out iterations in the calcium concentration and applied the trapezoidal rule. A uniform grid with a radial step $\Delta r = 1.2 \times 10^{-3}$, time step $\Delta t = 1.2 \times 10^{-4}$, and iteration error 1×10^{-4} was used. As new initial conditions the disturbed stationary distributions (3.4) were assigned.

As a test solution in the case of passive dilatation of the artery, the exact solution (5.7) was taken. A comparison shows good agreement between the numerical and exact solutions (Fig. 4).

In response to a change in the average blood flow-rate, determined by the coefficient $\psi_0' \sim Q$ in kinetic equation (2.19), as a result of damping of the oscillations the system goes over into a new equilibrium state (Fig. 5). In the calculations we used the characteristic parameter values given in the table, the elastic modulus $E_0 = 0.15 \times 10^5$ Pa, and the pressure $P_0 = 2 \times 10^4$ Pa $\simeq$ 150 mm Hg.

The characteristic period of the slow radius oscillations observed is equal to about 50 s. This is consistent with the experimentally obtained oscillation frequencies due to endothelium-dependent regulation, which
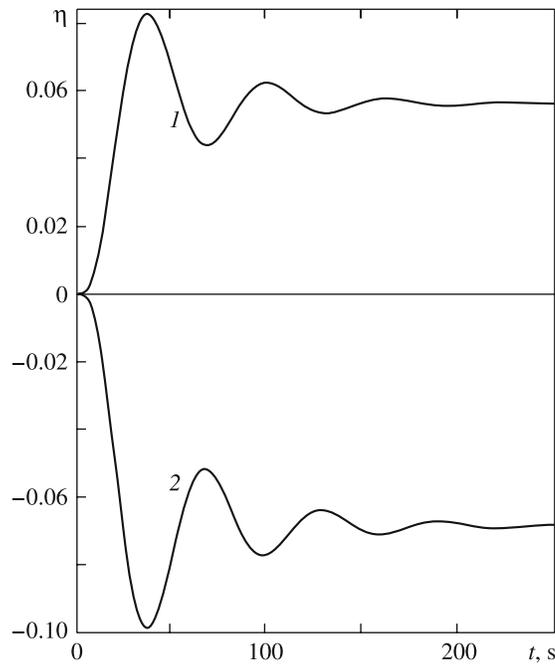
Fig. 5. Time dependence of the relative change in the artery radius η with increase (*1*) and decrease (*2*) in the average blood flow-rate by 25%.

vary on the range 0.01–0.1 Hz [31]. These oscillations are determined not by the characteristic frequencies of the natural mechanical oscillations of the artery but by the characteristic times of the kinetic processes in the vessel wall, that is, are modulated by the active muscular contraction.

It is noteworthy that the system response to a change in the flow-rate may differ. The relaxation times corresponding to an increase and a decrease in the blood flow-rate are not the same. This is attributable to the flow-rate dependence of the width of the interval of the arterial-wall viscosity parameter β on which the system is linearly stable in accordance with (4.5). The artery radius deviation is somewhat greater in the case of flow-rate decrease due to the inverse cubic dependence of the shear stress on the radius.

We will compare the numerical results with the experimental data [30]. In this experiment on anesthetized dogs the quantitative relationship between an increase in the blood flow-rate and the artery diameter was determined. The artery diameter was measured at two points on the artery. At one of these the endothelial layer was artificially damaged, whereas at the other it was left intact. The average pressure P_0 was maintained constant.

At the site with an intact endothelium the effect of both a short-term (less than 1 min) and a sustained (more than 3 min) increase in the blood flow-rate on the artery diameter was observed and recorded, whereas at the site with a damaged epithelial layer the diameter variations were negligible and related with small variations of the transmural pressure [30].

A sustained (3–4 min) increase in the average blood flow-rate level from 104.7 ± 15.1 to 694.7 ± 135.1 ml/min led to an increase in the outside diameter from the reference value 4.89 ± 0.12 mm to 5.37 ± 0.10 mm. The corresponding experimental data are presented in Fig. 5 in [30].

The characteristic data used in the numerical simulation of the autoregulation process are given in the table. In addition, we used the following parameter values: $k_1 = 0.015$ s^{-1}, $\varphi_0 = 0.00581$ μmol/s, $C_{th} = 0.1$ μmol, $n_0 = 1$ μmol, $\gamma = 10$ s^{-1}, $\xi = 0.5$, $\varepsilon = 0.1$, $t_0 = 10$ s, and $\lambda = 0.1 E_0 t_0 / R_0$ kg m^{-2} s^{-1}.

The numerically calculated time dependence of the average diameter with increase in the average blood flow-rate is shown in Figs. 6 and 7 for model parameters corresponding to the experimental conditions [30]. An almost sevenfold increase in the blood flow-rate in accordance with the hyperbolic-tangent law gave a relative increase in the inner artery radius of about 12%. The time lag in the vessel wall relaxation (Fig. 6b)
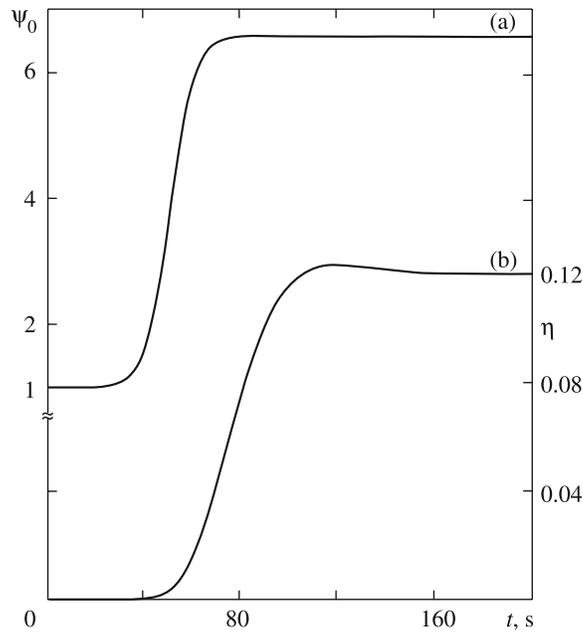
Fig. 6. Time dependence of the relative change in the radius of the external iliac artery (b) during a prolonged change in the average blood flow-rate level (a) (numerical calculation).
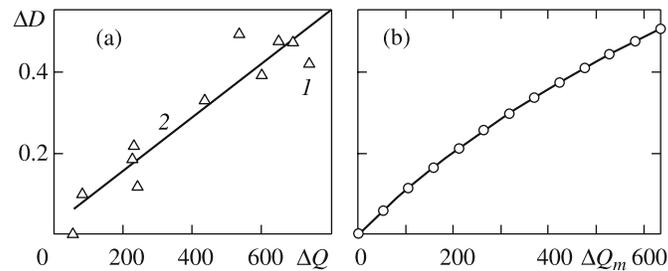
Fig. 7. Comparison of the experimental and numerical dependences of the change in artery diameter (mm) on the change in blood flow-rate (ml/min): (a) experimental data [30] ((*1*) measurement data, (*2*) linear regression), (b) mathematical modeling of the local autoregulation process (symbols denote the data of a series of calculations).

in response to an increase in the blood flow-rate (Fig. 6a) is equal to about 20 s and consistent with the experimental data [5, 16, 30].

In Fig. 7 the experimental dependence of the variation of the outer diameter ΔD on the maximum blood flow-rate in the dog external iliac artery with intact endothelium obtained in [30] (Fig. 7a) is compared with the dependence of ΔD on the average flow-rate obtained numerically under similar conditions (Fig. 7b).

The average slope of the numerically obtained flow-rate dependence of the vessel diameter is equal to 0.8×10^{-3} mm ml^{-1} min, which is consistent with the experimental data $0.83 \pm 0.15 \times 10^{-3}$ mm ml^{-1} min obtained in [30] using linear regression analysis.

We note that in Fig. 7 the numerical dependence is weakly nonlinear and similar in shape to the cube-root function, which may be attributed to the tendency to maintain a constant shear stress on the inner surface during blood flow.

Summary. For describing the local arterial autoregulation process due to the shear stress a two-layer diffusion-kinetic model is proposed.

In the stationary case, accurate distributions of the concentrations of the key agents: nitric oxide, calcium ions, and phosphorylated myosin, are found.

The limiting case of a thin-walled artery is studied analytically. A sufficient condition of stability of the dynamic system that describes autoregulation is obtained. The importance of viscoelasticity in ensuring the stability of the system equilibrium state is demonstrated.

In the case of complete relaxation of the artery wall muscles, an exact solution in the form of a transition wave, which describes the passive artery dilatation, is found. This case of complete wall muscle relaxation may be realized when nitric oxide donors, such as nitroglycerine and sodium nitroprusside, are introduced into the blood flow.

Using a numerical simulation, the transition of the system to a new equilibrium state with a new radius value in response to a change in the blood flow-rate level is investigated. The presence of a time lag in the artery response is shown. The numerical results are consistent with the experimental data.

REFERENCES

1. S. Čanic and A. Mikeli, "Equations Modeling the Flow of a Viscous Incompressible Fluid through a Long Elastic Tube Arising in the Study of Blood Flow through Small Arteries," SIAM J. Appl. Dynam. Systems **2** (3), 431–463 (2003).
2. G. Pontrelli and E. Rossoni, "Numerical Modelling of the Pressure Wave Propagation in the Arterial Flow," Int. J. Num. Meth. Fluids **43** (6–7), 651–671 (2003).
3. L. Formaggia, D. Lamponi, and A. Quarteroni, "One-Dimensional Models for Blood Flow in Arteries," J. Eng. Math. **47** (3–4), 251–276 (2003).
4. A.A. Bykova and S.A. Regirer, "Mathematical Models in Urinary System Mechanics (Review)," Fluid Dynamics **40** (1), 1–19 (2005).
5. H.M. Snow, F. Markos, D. O'Regan, and K. Pollock, "Characteristics of Arterial Wall Shear Stress which Cause Endothelium-Dependent Vasodilatation in the Anaesthetized Dog," J. Physiology **531** (3), 843–848 (2001).
6. J.E. Buchanan and J.W. Phillis, "The Role of Nitric Oxide in the Regulation of Cerebral Blood Flow," Brain Res. **610** (2), 248–255 (1993).
7. A. Rachev, "A Model of Arterial Adaptation to Alterations in Blood Flow," J. Elasticity **61** (1–3), 83–111 (2000).
8. K.M. Smith, L.C. Moore, and H.E. Layton, "Advective Transport of Nitric Oxide in a Mathematical Model of the Afferent Arteriole," Amer. J. Physiol. **284** (5), F1080–1096 (2003).
9. S.A. Regirer and N.Kh. Shadrina, "Elementary Model of a Blood Vessel with a Wall Sensitive to Mechanical Stimuli," Biofizika **47** (5), 908–913 (2002).
10. F. Kappel and R.O. Peer, "A Mathematical Model for Fundamental Regulation Processes in the Cardiovascular System," J. Math. Biology **31** (6), 611–631 (1993).
11. M.S. Olufsen, J.T. Ottesen, H.T. Tran, et al., "Blood Pressure and Blood Flow Variation during Postural Change from Sitting to Standing: Model Development and Validation," J. Appl. Physiol. **99** (4), 1523–1537 (2005).
12. J. Lancaster, Jr., "Simulation of the Diffusion and Reaction of Endogeneously Produced Nitric Oxide," PNAS **91** (17), 8137–8141 (1994).
13. M.W. Vaughn, L. Kuo, and J.C. Liao, "Effective Diffusion Distance of Nitric Oxide in the Microcirculation," Amer. J. Physiol. Heart. Circ. Physiol. **274** (5), H1705–1714 (1998).
14. R. F. Furchgott and J. V. Zawadzki, "The Obligatory Role of Endothelial Cells in the Relaxation of Arterial Smooth Muscle by Acetylcholine," Nature **288** (5789), 373–376 (1980).
15. R.F. Furchgott, "Endothelium-Derived Relaxing Factor: Discovery, Early Studies, and Identification as Nitric Oxide," Biosci. Rep.**19** (4), 235–251 (1999).
16. A.M. Melkumyants and S.A. Balashov, *Mechanosensitivity of the Arterial Endothelium* [in Russian] (Triada, Tver, 2006).
17. S. Payne, H. Morris, and A. Rowley, "A Combined Haemodynamic and Biochemical Model of Cerebral Autoregulation," in *Proc. 27th IEEE EMBS Conf. Shanghai, China* (2005).
18. R. Joannides, W.E. Haefeli, L. Linder, et al., "Nitric Oxide is Responsible for Flow-Dependent Dilatation of Human Peripheral Conduit Arteries in Vivo," Circulation **91** (5), 1314–1319 (1995).
19. G.M. Rubanyi, J.C. Romero, and P.M. Vanhoutte, "Flow-Induced Release of Endothelium-Derived Relaxing Factor," Amer. J. Physiol. Heart. Circ. Physiol. **250** (6), H1145–1149 (1986).

20. C.G. Caro, T.J. Pedley, R.C. Schroter, and W.A. Seed, *The Mechanics of the Circulation* (Univ. Press, Oxford, 1978).

21. Y.C. Fung, *Biomechanics: Mechanical Properties of Living Tissues* (Springer–Verlag, Berlin, 1993).

22. S.A. Regirer and N.Kh. Shadrina, 'Mathematical Models of Nitric Oxide Transport in a Blood Vessel," Biofizika **50** (3), 515–536 (2005).

23. A. Kamiya and T. Togawa, "Adaptive Regulation of Wall Shear Stress to Flow Change in the Canine Carotid Artery," Amer. J. Physiol. Heart. Circ. Physiol. **239** (1), H14–21 (1980).

24. N.A. Kudryashov and I.L. Chernyavskii, "Nonlinear Waves in Fluid Flow through a Viscoelastic Tube," Fluid Dynamics **41** (1), 49–62 (2006).

25. T.J. Pedley, "Mathematical Modelling of Arterial Fluid Dynamics," J. Eng. Math. **47** (3–4), 419–444 (2003).

26. R.C. Dorf, *CRC Handbook of Engineering Tables* (CRC Press, 2003).

27. J.K.-J.Li, *Dynamics of The Vascular System* (World Scientific, N.Y., 2004).

28. N.A. Kudryashov, "Simplest Equation Method to Look for Exact Solutions of Nonlinear Differential Equations," Chaos, Solitons and Fractals **24** (5), 1217–1231 (2005).

29. N.A. Kudryashov, "Exact Solutions of the Generalized Kuramoto–Sivashinsky Equation," Phys. Lett. A **147** (5–6), 287–291 (1990).

30. H. Snow, S. McAuliffe, J. Moors, and R. Brownlie, "The Relationship between Blood Flow and Diameter in the Iliac Artery of the Anaesthetized Dog: the Role of Endothelium-Derived Relaxing Factor and Shear Stress," Exp. Physiol. **79** (5), 635–645 (1994).

31. *Laser Doppler Flowmetry of Blood Microcirculation* [in Russian], Ed. by A.I. Krupatkin and V.V. Sidorov (Meditsina, Moscow, 2005).